

1 The bacterial genetic determinants of *Escherichia coli* 2 capacity to cause bloodstream infections in humans

3 Judit Burgaya^{1,2*}, Julie Marin^{3*}, Guilhem Royer^{4,5,6}, Bénédicte Condamine⁴, Benoit Gachet⁴,
4 Olivier Clermont⁴, Françoise Jaureguy³, Charles Burdet⁴, Agnès Lefort⁴, Victoire de
5 Lastours⁴, Erick Denamur^{4,7†}, Marco Galardini^{1,2†}, François Blanquart^{8†} and the
6 Colibafi/Septicoli and Coliville groups#

7

8 * co-first authors

9 † co-last authors

10 # The names of the collaborators are listed in the Acknowledgement section.

11

12 ¹ Institute for Molecular Bacteriology, TWINCORE Centre for Experimental and Clinical
13 Infection Research, a joint venture between the Hannover Medical School (MHH) and the
14 Helmholtz Centre for Infection Research (HZI), Hannover, Germany

15 ² Cluster of Excellence RESIST (EXC 2155), Hannover Medical School (MHH), Hannover,
16 Germany

17 ³ Université Sorbonne Paris Nord, INSERM, IAME, 93000 Bobigny, France

18 ⁴ Université Paris Cité, INSERM, IAME, 75018 Paris, France

19 ⁵ Département de Prévention, Diagnostic et Traitement des Infections, Hôpital Henri Mondor,
20 94000 Créteil, France

21 ⁶ Unité Ecologie et Evolution de la Résistance aux Antibiotiques, Institut Pasteur, UMR
22 CNRS 6047, Université Paris-Cité, 75015 Paris, France

23 ⁷ Laboratoire de Génétique Moléculaire, Hôpital Bichat, AP-HP, 75018 Paris, France

24 ⁸ Center for Interdisciplinary Research in Biology, Collège de France, CNRS UMR7241 /
25 INSERM U1050, PSL Research University, Paris 75005, France

26

27 Corresponding author: Erick Denamur, erick.denamur@inserm.fr

28 Abstract

29 *Escherichia coli* is both a highly prevalent commensal and a major opportunistic pathogen
30 causing bloodstream infections (BSI). A systematic analysis characterizing the genomic
31 determinants of extra-intestinal pathogenic vs. commensal isolates in human populations,
32 which could inform mechanisms of pathogenesis, diagnostics, prevention and treatment is still
33 lacking. We used a collection of 1282 BSI and commensal *E. coli* isolates collected in France
34 over a 17-year period (2000-2017) and we compared their pangenomes, genetic backgrounds
35 (phylogroups, STs, O groups), presence of virulence-associated genes (VAGs) and
36 antimicrobial resistance genes, finding significant differences in all comparisons between
37 commensal and BSI isolates. A machine learning linear model trained on all the genetic
38 variants derived from the pangenome and controlling for population structure reveals similar
39 differences in VAGs, discovers new variants associated with pathogenicity (capacity to cause
40 BSI), and accurately classifies BSI vs. commensal strains. Pathogenicity is a highly heritable
41 trait, with up to 69% of the variance explained by bacterial genetic variants. Lastly,
42 complementing our commensal collection with an older collection from 1980, we predict that
43 pathogenicity increased steadily from 23% in 1980 to 46% in 2010. Together our findings
44 imply that *E. coli* exhibit substantial genetic variation contributing to the transition between
45 commensalism and pathogenicity and that this species evolved towards higher pathogenicity.

46 Introduction

47 *Escherichia coli* bloodstream infections (BSI) are severe diseases with an incidence of around
48 5×10^{-4} to 1×10^{-3} per person-year in Europe and the United States (1–5) and a mortality
49 ranging from 10 to 30% (5), and may account for a few percents of all deaths in these
50 countries (4). The increase in incidence of BSI (1, 2), the global emergence of multidrug
51 resistance clones such as ST131 (6–9), and the ageing population all make BSI an important
52 and growing public health problem. A better understanding of the bacterial genetic factors
53 determining pathogenicity (the capacity to cause infection) and virulence (the severity of
54 infection) (10) would improve our understanding of pathophysiology and potentially improve
55 stewardship and control policies.

56 The primary niche of *E. coli* is the gut of vertebrates, especially humans, where it behaves as
57 a commensal (11). BSI are opportunistic infections. Two main routes of infection are
58 described, digestive and urinary, corresponding to two distinct pathophysiologic entities. BSI
59 with a digestive portal of entry are more severe. Host condition and comorbidities affect
60 virulence (12–14). A few bacterial genetic factors affecting virulence have been reported. In a
61 genome-wide association study (GWAS) conducted on 912 patients, no bacterial genetic
62 factor was associated with outcome (death, septic shock, admission to ICU), possibly because
63 of insufficient power. Alternatively, in a murine model of BSI, a GWAS conducted on 370
64 *Escherichia* strains have shown that the *Yersinia pestis* High Pathogenicity Island (HPI), and
65 two additional groups of genes involved in iron uptake, were associated with a higher
66 probability of mouse death (15).

67 There is a rich tradition of comparing *E. coli* strains sampled from commensal carriage vs. in
68 infections to reveal the determinants of pathogenicity (16, 17). These studies often do not
69 sequence full genomes, which prevents the control for bacterial population structure and the
70 discovery of new determinants of pathogenicity beyond already established lists of virulence
71 genes. Moreover, many studies compare *E. coli* from stools vs. from infections in the same
72 individuals (16). This design is interesting because it blocks hosts factors. But it may also
73 have limited power to detect variants associated with infections because it conditions on
74 individuals *with* an infection, limiting the possibility of comparison to the diversity of strains

75 present in stools. So far, no studies investigated the bacterial genetic determinants of the
76 capacity to cause an infection by comparing large numbers of whole genome sequences of
77 bacteria sampled from the gut (commensals) vs. sampled from infections. This may be
78 explained in part by the small number of large commensal strain collections (18). Another
79 difficulty is that host factors, such as age or co-morbidities, are important determinants of
80 infection (19), and must be adjusted for as much as possible when comparing strains sampled
81 in the two contexts. Lastly, the increased availability of large whole genome sequence
82 collections from BSI also established that a small number of sequence types, mainly ST131,
83 73, 95, 69, 10, are involved in the majority of BSI (20). These STs are rich in virulence
84 associated genes (VAGs) encoding adhesins, iron acquisition systems, protectins and toxins
85 (16, 17), but pinpointing potentially causal individual genetic determinants can only be done
86 in a rigorous GWAS. So far, no systematic examination of the bacterial genetic determinants
87 of *E. coli* pathogenicity has been done by comparison with a large commensal collection.

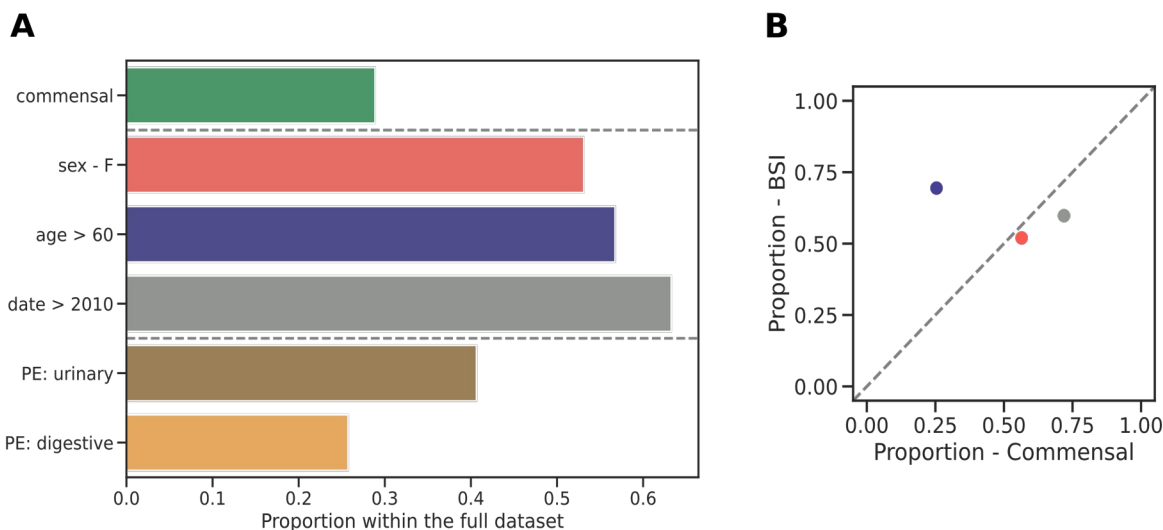
88 In the present work, we took advantage of two recently published collections of BSI (1) and
89 commensal (18) strains gathered between 2000 and 2017 in France and with their genome
90 sequenced. We compared BSI and commensal strain genomes at three levels: phylogenomic
91 composition, virulence and resistance gene content, and lastly unitig content in a GWAS. Our
92 goal was to compare the diversity of commensal and BSI strains and to identify specific
93 genomic features affecting the propensity to cause BSI, using both a targeted and a
94 hypothesis-free approach.

95 Results

96 A dataset of 912 BSI and 370 commensal isolates

97 We compared the genomes of 912 strains from BSI in adults, originating from two
98 prospective multicentric studies (Colibafi in 2005 and Septicoli in 2016-7 (19, 21)) performed
99 in the Paris area, to the genomes of 370 commensal strains gathered from stools of healthy
100 adult subjects in 2000, 2001, 2002, 2010 and 2017 in Brittany and the Paris area. In-hospital
101 death (or at Day 28) was 12.9 and 9.5% in the Colibafi and Septicoli studies, respectively.
102 Most of the BSI were community acquired (79.6 and 54.3% in the two collections,
103 respectively). To avoid biases, all strains were isolated with similar protocols adapted to the

104 sample origin (BSI and commensal) and sequenced in our laboratory using a similar approach
105 (Illumina technology). To reduce the influence of the origin of the different studies we
106 introduced the date of the study as a covariate, encoding it as a binary variable with the
107 studies collected before and in or after 2010. To account for host factors, we additionally
108 included sex and age as binary variables. For age, the variable was recording if the
109 donor/patient was above 60 years old or not. Finally, we also focused on the reported portal of
110 entry of the BSI strains, which has previously been associated with some genetic variants
111 (**Figure 1A**) (22). The two collections had similar distributions of these variables, with the
112 important exception of the proportion of isolates corresponding to older donors/patients,
113 which is higher (69.43%) in the BSI collection (**Figure 1B**).



114 **Figure 1. Variables of the combined dataset.** (A) Proportion of commensal isolates, distribution of covariates
115 (sex, age, collection date), and BSI isolates with the urinary tract and digestive tract as portal of entry within the
116 full dataset. (B) Scatter plot of the distributions of all covariates in the two collections, colors matching that of
117 panel A. PE: portal of entry.

118 **Commensal strains are genetically more diverse than BSI strains and have a distinct
119 phylogenetic composition**

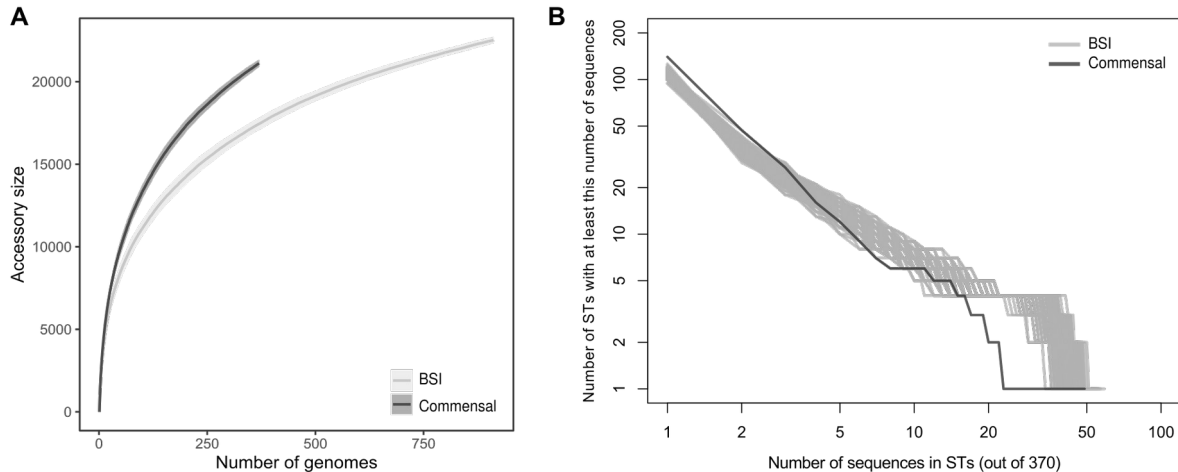
120 We first compared the global phylogenomic characteristics of the two collections. The
121 pangenomes of the BSI ($N = 912$) and commensal ($N = 370$) collections were composed of
122 24,321 and 22,373 genes, respectively. For a comparable number of strains, commensal

123 strains had a higher diversity in gene content than BSI strains (**Figure 2A**). Conversely, the
124 core genomes of both collections were similar (3133 and 2985 genes, respectively), and close
125 to the core genome of *E. coli* species as a whole. In terms of SNP diversity of the core
126 genome, the commensal collection was more diverse (pairwise nucleotide diversity $\pi = 2.10e-2$)
127 than the BSI collection ($\pi = 2.05e-2$, p-value < 2.2e-16).

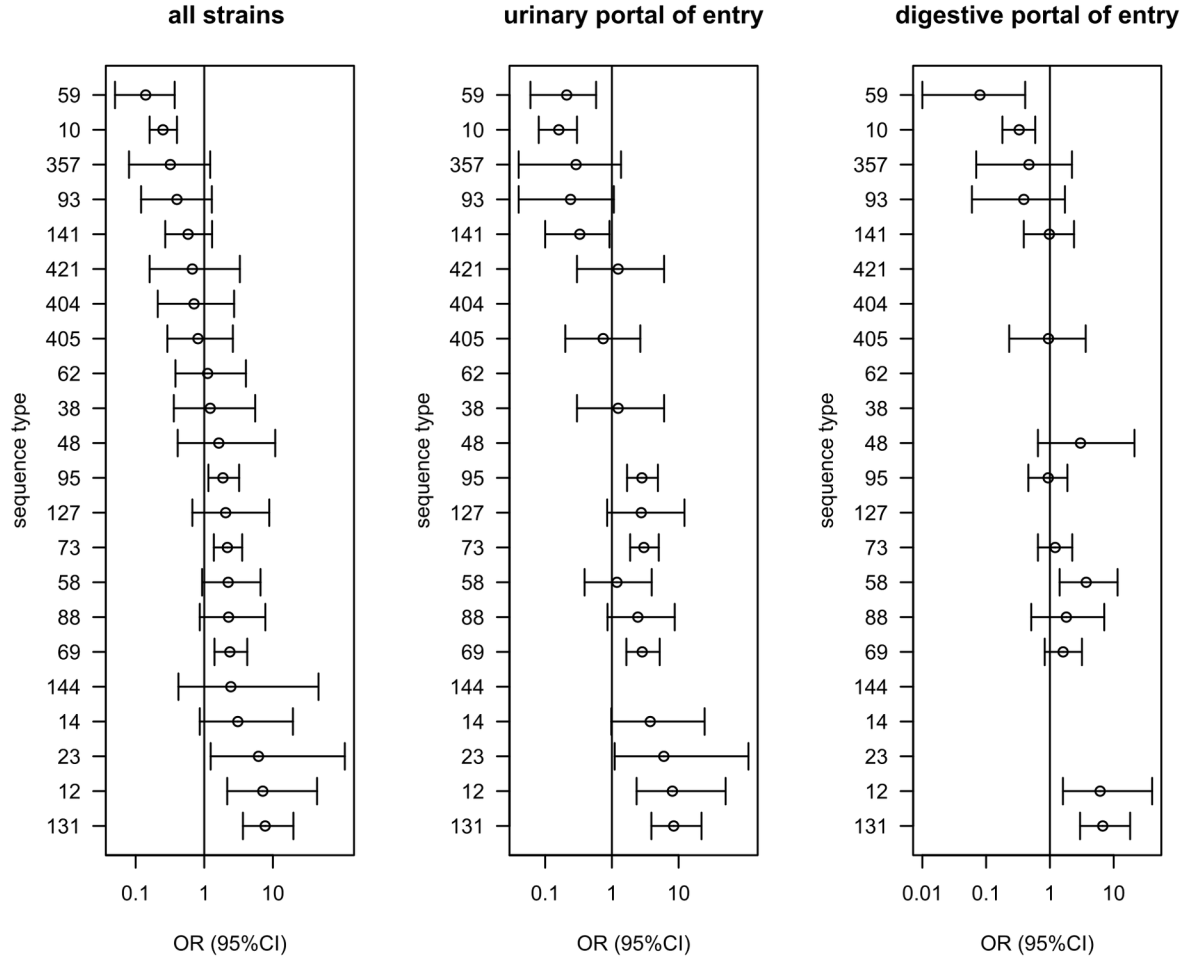
128 Commensal strains belong almost equally to A and B2 phylogroups (25.41% and 32.43%)
129 whereas BSI strains belonged mainly to phylogroup B2 (51.21%) followed by D phylogroup
130 (15.79%) (**Table S1**). The commensal collection was more diverse in its ST composition,
131 with a higher number of rare STs and a lower number of frequent STs compared to the BSI
132 collection (**Figure 2B**). This greater phylogenetic diversity could explain both the larger
133 diversity in gene content (23) and larger nucleotidic sequence diversity of the pangenomes of
134 commensals.

135 As previously noted, the diversity of STs in commensal strains was very distinct to that in BSI
136 strains (**Table S2**). Notably, ST10 and ST59 are abundant in commensal strains (13.2% and
137 3.8%) but under-represented in BSI strains (3.7% and 0.6%); on the contrary, ST131, ST73,
138 ST69, ST95 are less common in commensal strains than they are in BSI strains. This
139 comparison can be translated in an odds ratio for the risk of infection associated with gut
140 colonization by each ST, which can be seen as a quantitative measure of pathogenicity. The
141 sequence type ST131 is the most pathogenic and ST59 the least pathogenic (**Figure 3** and
142 **Table S2**). When the portal of entry was considered for the ST distribution, a similar pattern
143 was observed for both portals of entry as for the whole collection, although the significance
144 level of the risk of infection might change (**Figure 3** and **Table S2**).

145 The distribution of the O-group diversity also differed between the commensal and the BSI
146 collections (**Table S3**). The four O-groups targeted by the recently developed bioconjugate
147 vaccine ExPEC4V (24, 25), O1, O2, O6 and O25 are the most abundant O-groups in the BSI
148 collection. However, unlike the O-groups O6 and O25, the O-groups O1 and O2 are not
149 particularly associated with BSI strains (**Table S3**). In other words, these two O-groups are
150 frequent in BSI because they are the two most frequent O-groups in commensalism, but are
151 not particularly pathogenic.



152 **Figure 2.** (A) Pangenome sizes as a function of the number of genomes analyzed for the BSI (912 strains) and
153 commensal (370 strains) collections, showing the greater pan genome size of the commensal collection. (B)
154 Cumulative distribution of strain sequences within ST in commensal and BSI collections. To be able to compare
155 the BSI collection with the smaller commensal collection ($N = 370$), we extracted 200 random sub-samples of
156 370 sequences from the BSI collection (grey curves).

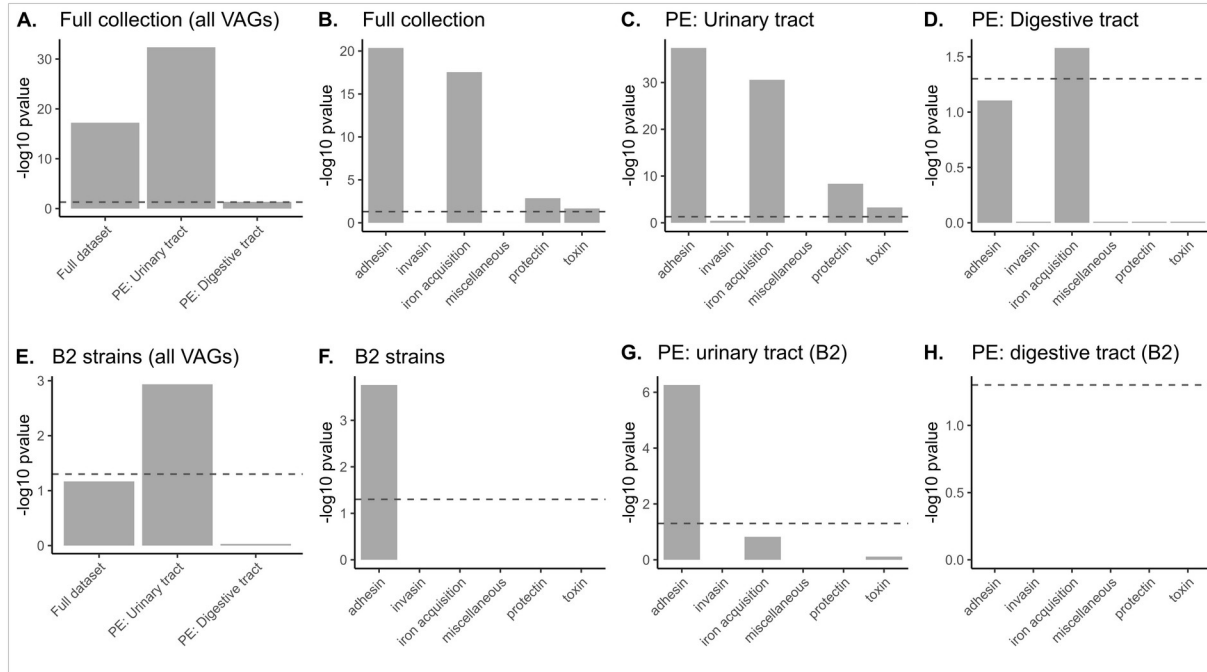


157 **Figure 3.** Comparison of the distribution of the sequence types (STs) of the *E. coli* commensal and BSI
158 collections isolates (see table S2). We show the odds ratio (OR with 95% CI) for the risk of infection associated
159 with colonization by each ST (logistic model of infection status as a function of the ST). We selected the STs
160 present in at least 5 strains in at least one of the two collections. STs are ordered by decreasing associated odd
161 ratio for all strains.

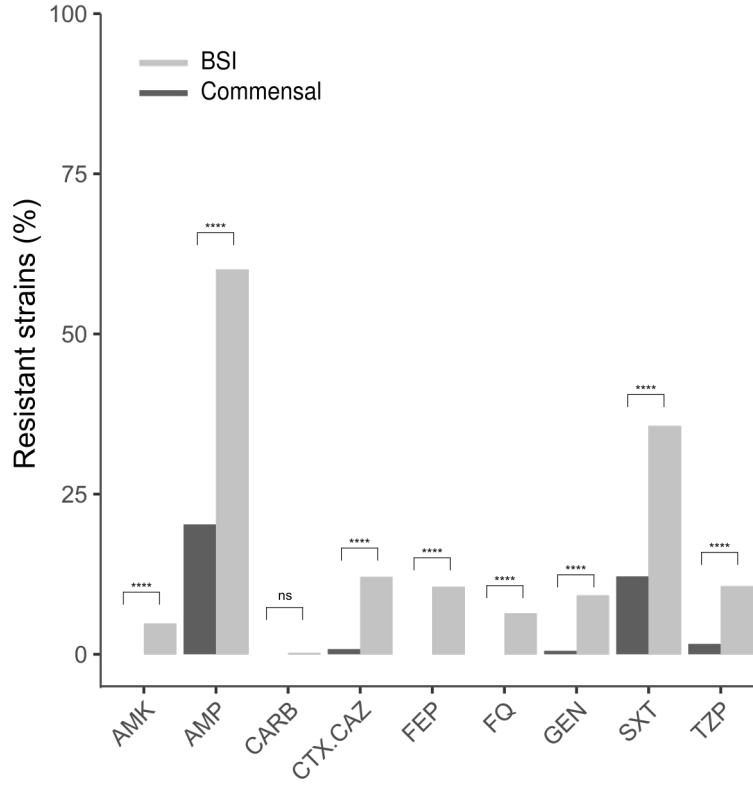
162 BSI strains are enriched in VAGs and antibiotic resistance genes (ARGs) as compared
163 to commensal strains

164 Using a targeted approach, we next focused on the frequency of VAGs and ARGs in both
165 collections. A global comparison in the number of VAGs classified in functional categories
166 showed a significantly higher presence of VAGs coding for adhesins, iron acquisition
167 systems, protectins and toxins categories in BSI strains (**Figure 4A and B, Figure S1, Table**
168 **S5**). We found similar results when comparing against BSI strains with urinary portal of entry
169 to commensals (**Figure 4C**). However, only the iron acquisition systems category remained

170 significant when comparing against BSI strains with digestive portal of entry (**Figure 4D**).
171 More precisely for the full dataset, the highest significance was observed for the *pap* genes
172 with the *papGII* allele, followed by the *sit*, *iuc* and *irp2/fyuA* (HPI) genes, all with p-values
173 $\ll 10^{-10}$ (**Table S5**). These analyses do not imply a causal role of these genes and alleles in
174 BSI, as they are not adjusted for the distinct phylogenomic composition of commensal and
175 BSI strains. However, it is possible to crudely adjust for this population structure by focusing
176 on the B2 phylogroup strains which are known to exhibit the highest prevalence of VAGs
177 within the *E. coli* species (17).
178 When only B2 phylogroup strains are compared, only VAGs coding for adhesins category
179 remained significantly over-represented in BSI (**Figure 4F**). When comparing only B2 strains
180 with urinary portal of entry to B2 commensals, again only adhesins were over-represented,
181 and no differences were observed when comparing only against B2 strains with digestive
182 portal of entry (**Figure 4G-H**). Regarding individual genes, interestingly, for two VAGs with
183 experimentally validated role in urinary tract infection, *pap* genes (26) and *fim* genes (27), we
184 found a higher level of significance in B2 strains with urinary portal of entry than in all B2
185 strains (*pap*) or in all strains (*fimD-H*) (**Table S5**).
186 BSI strains were predicted to be more resistant to all classes of antibiotics than commensal
187 strains (**Figure 5**). The only exception was for carbapenems (for which resistance was
188 predicted to be very rare). This also holds true if specific portals of entry and/or phylogroup
189 B2 are taken into account (**Figure S2**). To verify that this over-representation of resistance in
190 BSI was not explained by the fact that BSI isolates are slightly more recent on average than
191 commensal isolates, we restricted our analysis to BSI Colibafi strains (sampled in 2005) and
192 found the same results when considering all phylogroups and portals of entry.
193 No difference in VAG numbers (t-test, all Benjamini-Hochberg corrected p value > 0.05), nor
194 in resistance prevalences (Fisher's exact test, all Benjamini-Hochberg corrected p value $>$
195 0.05), was found when comparing nosocomial and community BSI strains, considering both
196 Septicoli (167 nosocomial and 296 community BSI strains) and Colibafi (75 nosocomial and
197 292 community BSI strains) collections together or individually.
198
199



200 **Figure 4.** Difference in the number of VAGs per strain among the six main functional classes of virulence
201 between the 912 BSI and 370 commensal strains (Benjamini-Hochberg corrected p value < 0.05). We tested
202 whether the number of VAGs was larger in BSI than in commensal strains considering (A-B) all the strains (912
203 BSI strains), (C) BSI strains with urinary portal of entry (PE) to commensals (498 BSI strains), (D) BSI strains
204 with digestive portal of entry to commensals (310 BSI strains), (E-F) the B2 strains (467 BSI strains), (G) B2
205 BSI strains with urinary portal of entry to commensals (304 BSI strains) and (H) B2 BSI strains with digestive
206 portal of entry to commensals (124 BSI strains). The dashed line represents the significance threshold at the 0.05
207 level.

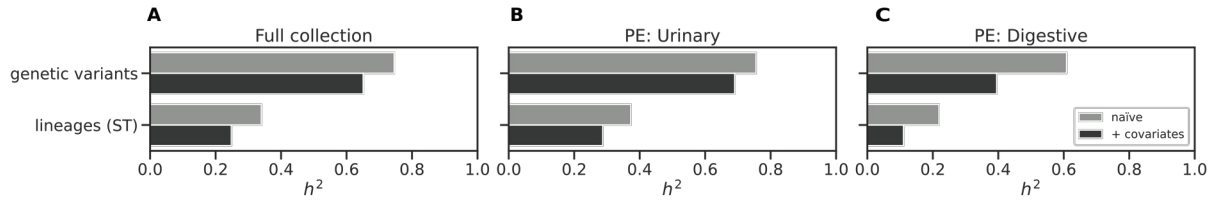


208 **Figure 5.** Predicted antibioresistance phenotypes of the 1282 strains (Benjamini-Hochberg corrected p value < 209 0.05). The results are presented as percentages of resistant strains for nine antibiotics of clinical importance. 210 AMK, amikacin; AMP, ampicillin; CARB, carbapenem; CTX/ CAZ, cefotaxime/ceftazidime; FEP, cefepime; 211 FQ, fluoroquinolones; GEN, gentamicin; SXT, cotrimoxazole; TZP, piperacillin/tazobactam.

212 Bacterial genetic factors explain a large fraction of the variation in the BSI phenotype

213 We computed the heritability, as the proportion of the variance of a phenotype explained by 214 variable genetic factors (28), to estimate whether we could expect to find bacterial genetic 215 variants associated with commensalism or BSI in our dataset. We first measured the 216 heritability using the ST information alone, to measure the influence of the genetic 217 background on phenotypic variability. We then computed the heritability emerging from the 218 individual genetic variants (Figure 6). We found that STs could explain 24%, 28%, and 11% 219 of the phenotypic variance in the full collection, the subset with BSI isolates with urinary tract 220 as portal of entry and digestive tract as portal of entry, respectively. Genetic variants alone 221 could explain a larger fraction of the phenotypic variability: 65%, 69%, and 39% for the three

222 subsets, respectively. This suggests that pathogenicity might not be solely determined by a
223 strains' genetic background but also through specific genetic determinants.

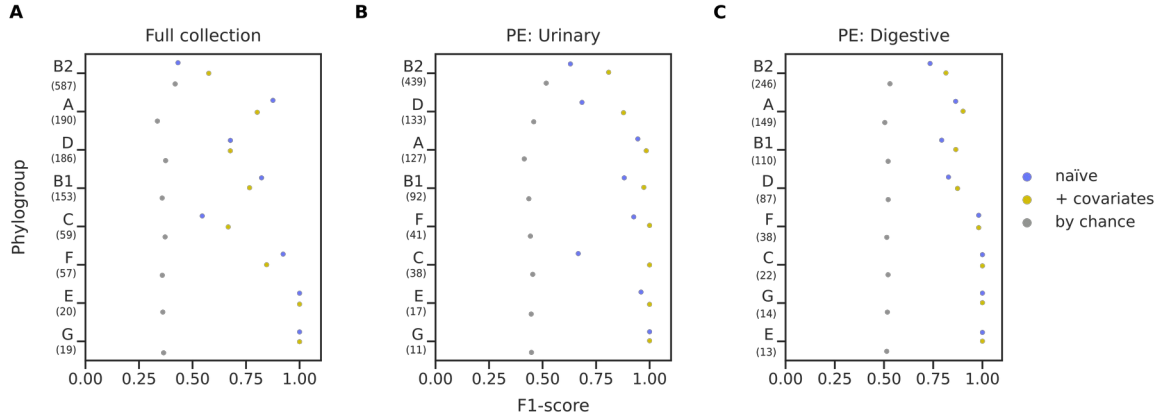


224 **Figure 6. Heritability estimates for the commensal phenotype.** A) Heritability estimates for the full dataset.
225 B) Heritability estimates for the subsets with BSI isolates with portal of entry as urinary tract and C) digestive
226 tract.

227 [A whole-genome machine learning model differentiates commensals from BSI strains](#)

228 We next applied a machine learning model trained on both the core and accessory genome of
229 the strains to differentiate between commensal and BSI strains and highlight the genetic
230 variants that contribute the most to the discriminatory power of the model (wg-GWAS). We
231 performed the analysis on three different datasets: the full strain collection, and two subsets of
232 BSI isolates: one with urinary tract as portal of entry, and another one with digestive tract as
233 portal of entry. We used all the genetic variants covering the pangenome compactly
234 represented by unitigs and the elastic net linear model implemented in pyseer for the
235 associations (29). We looked for associations between genetic variants and whether a strain
236 was classified as a commensal as the phenotype, and used the following three binary variables
237 as covariates to account for host factors and collection biases: the sex of the donor/patient,
238 their age (older than 60 years old), and the date of each collection (before or after 2010). To
239 quantify model performance, we performed a cross validation by holding out one phylogroup
240 at a time, and computed the precision (proportion of true BSI among the predicted BSI
241 strains), recall (sensitivity) and F1-score (harmonic mean of precision and recall) (**Figure 7**
242 **and S3**). The model performance improved in all cases when the covariates were considered
243 for the associations, potentially confirming that host factors also explain part of bacterial
244 pathogenicity. We also found a better model performance in the two subsets with BSI isolates
245 with a specific portal of entry, compared to the full collection, which could underscore the
246 presence of specific genetic variants associated with either portal of entry.

247



248 **Figure 7. wg-GWAS model performance. F1-score representation** (a) For the full collection (b) the subset of
249 clinical isolates with urinary tract as portal of entry, and (c) the subset of clinical isolates with digestive tract as
250 portal of entry, for the naive analysis (blue dots), with covariates (yellow dots), and the one expected by chance
251 (grey dots). Numbers within parenthesis below each phylogroup indicates the sample size.

252 We found a number of unitigs to be associated with commensalism (*i.e.* with non-zero weight
253 in the elastic net model). Overall, 107 and 59 unitigs passed the threshold for the model built
254 naïvely and with covariates, respectively, which we then mapped back to 34 and 28 genes.
255 We found that 8 out of the 28 genes obtained through the analysis with covariates were
256 clearly related to virulence. We found the *iucB* gene, encoding an aerobactin siderophore
257 biosynthesis protein (30) and *papG* encoding the adhesin at the tip of the P pilus (31). Both
258 have already been associated with invasive uropathogenic *E. coli* (UPEC) isolates (22, 32). Of
259 note, these genes were identified using the targeted approach after adjusting for population
260 structure by focusing on the B2 phylogroup strains (see above). We also found the following
261 genes: *sopB* which is an inositol phosphate phosphatase associated to virulence in *Salmonella*
262 (33); *mltB*, which is part of a network connecting resistance, membrane homeostasis,
263 biogenesis of pili and fitness in *Acinetobacter baumannii* (34); *fliL*, encoding for the flagellar
264 protein FliL (35). And lastly, two unnamed orthologous groups (group_5900 and
265 group_9261), described as the putative bacterial toxin *ydaT* (36). We found more genes
266 associated to the phenotype when dividing the BSI strains according to their portal of entry.
267 We found a total of 152 and 96 associated unitigs for the urinary and digestive tract subsets,
268 respectively, which we then mapped back to 101 and 45 genes, some of which are known to
269 be involved in pathogenicity and antimicrobial resistance (**Table 1 and S6**). Taken as a
270 whole, we found the associated genes to be enriched in the L COG category (replication,

271 recombination and repair) for the three subsets, and in the K COG category (transcription) for
272 the full dataset only. We also performed a Gene Ontology (GO) term enrichment analysis and
273 found that for the subset with BSI isolates with urinary tract as portal of entry, the relevant
274 (depth > 1) enriched GO terms include different categories related to metabolic processes, ion
275 binding and intracellular anatomical structure (**Table S7**). Similarly, to the targeted analysis
276 described above, we found that the genes resulting from the three associations were enriched
277 for VAGs and ARGs (**Figure 8**); when considering all VAGs and ARGs together we found a
278 significant (pvalue < 0.05) enrichment for the full dataset and the urinary tract subset. We
279 found VAGs related to iron acquisition to be enriched in all three datasets, while adhesins
280 were enriched in the full dataset only. For the ARGs, only the resistance to cotrimoxazole
281 (dfrA for SXT resistance) was enriched in the urinary tract subset.

282 The model can be used to predict the potential pathogenicity of other isolates based on the
283 presence of the unitigs for which the model's weight is different than zero. We predicted the
284 pathogenicity of commensal strains collected at three time periods: 1980 (37), 2000-2002 and
285 2010. Interestingly, the model predicts a marked increase in pathogenicity of these
286 commensal isolates, with the proportion doubling between the 1980s and the 2010s (23% vs.
287 46%, **Figure S4**). This suggests that the commensal strains inhabiting the gut of healthy
288 humans may have evolved towards higher pathogenicity in the past decades.

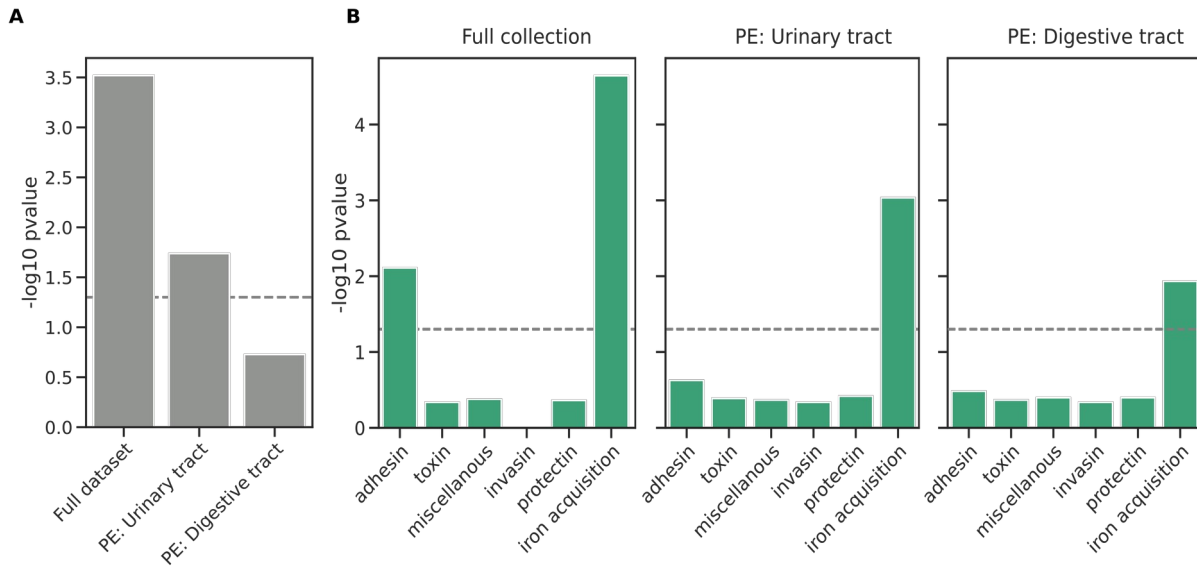
289 Through an unbiased approach based on the whole pangenome, we have drawn similar results
290 as a more targeted approach, namely that VAGs are to some extent able to distinguish
291 commensals from pathogenic isolates.

292 **Table 1** Genes with functions related to pathogenicity and antimicrobial resistance with
293 unitigs associated with the phenotype mapped to them for the two subsets.

Portal of entry: urinary tract

Gene	Relevance	Reference
<i>papG</i>	Adhesin. Belongs to the pap operon encoding for a type P pilus.	(22, 31)
<i>papH</i>	Adhesin VAG. Belongs to the pap operon encoding for a type P pilus.	(32)
<i>iucB/C</i>	Iron acquisition VAG. Aerobactin siderophore biosynthesis protein	(30)
<i>sopB</i>	inositol phosphate phosphatase associated to virulence in	(33)

<i>Salmonella</i>		
<i>mltC</i>	Involved in release of peptidoglycan-derived pathogen-associated molecular patterns as a virulence mechanism	(38)
<i>ompX</i>	Might be involved in biofilm formation and curli production	(39)
<i>dhfrI</i>	Trimethoprim resistance gene	(40)
<i>fliD</i>	Relevance in adhesion. Flagellar hook-associated protein.	(41)
<i>dgcE</i>	Involved in regulation of the switch from flagellar motility to sessile behavior and curli expression	(42)
Groups 10969 and 4151	Type II/IV secretion system protein (T2SSE)	Table S8
Group 9261	Putative bacterial toxin	Table S8
<i>epsM</i>	Involved in type II secretion systems (T2SS)	Table S8
<i>aceF</i>	Involved in the virulence and oxidative response of <i>P.aeruginosa</i> .	(43)
<i>klcA</i>	Present in the <i>kilC</i> operon found in IncP plasmids, which usually carry multiple AMR determinants.	(44)
Portal of entry: digestive tract		
Gene	Relevance	Ref
<i>iucC</i>	Iron acquisition VAG. Aerobactin siderophore biosynthesis protein	(30)
Group 3130	Tfp pilus assembly protein FimV	Table S8
<i>fliD</i>	Relevance in adhesion. Flagellar hook-associated protein.	(41)
<i>sopB</i>	inositol phosphate phosphatase associated to virulence in <i>Salmonella</i>	(33)
<i>epsE/F</i>	Type II/IV secretion system protein	Table S8
<i>yehB</i>	Relevance in adhesion. Encodes a type of putative fimbrial complex belonging to the chaperone-usher assembly pathway.	(45)



294 **Figure 8.** A) Virulence associated genes enrichment analysis for the full set of genes and B) the different
295 functional categories. The significance threshold is represented over the dotted line (Fisher's exact test, $p < 0.05$).
296 PE: portal of entry.

297 Discussion

298 It is known since the 1940s (46) that within the *E. coli* species, some strains with a specific
299 genetic background have higher capacity to cause extra-intestinal diseases. Later on,
300 pathogenicity has been associated with specific serotypes, STs, and the phylogroup B2, which
301 are enriched in some VAGs (47, 48). However, disentangling the respective roles of causal
302 genetic variants from the genetic background in a mostly clonal species is a difficult task (49).
303 To do so, we systematically investigated the genomic differences between 912 *E. coli* strains
304 from bloodstream infections and 370 strains sampled from the stools of healthy volunteers.

305 We revealed differences at three levels. First, at the phylogenetic level, strains from BSI are
306 less diverse, dominated by a small number of highly pathogenic STs, and have consequently
307 smaller pangenomes and lower genetic diversity than commensal strains. Second, strains from
308 infections are enriched in VAGs, and are predicted to be more antibiotic resistant. Third, in a
309 machine learning assisted GWAS, we found 101 and 45 genes associated with BSI with
310 urinary and digestive portal of entry, respectively, independently of the clonal background.
311 Some of these are involved in adhesion and in iron acquisition, as well as other functions.
312 Generally, genes with a significant association are enriched in iron acquisition system, the L

313 COG category (replication, recombination and repair) and GO terms including different
314 categories related to metabolic processes, ion binding and intracellular anatomical structure.
315 The heritability of pathogenicity is estimated at 69% (urinary PE) and 39% (digestive PE), in
316 agreement with the higher role of the host factors in BSI with digestive PE (19, 21). Thus, a
317 large fraction of pathogenicity is explained by bacterial genetic factors. This is roughly double
318 of the heritability when considering STs alone, suggesting that specific genetic variants at a
319 finer phylogenetic scale than ST are determining pathogenicity. For comparison, age, a host
320 factor strongly associated with BSI, explains 17.6% of the variance. Thus, we conclude that
321 bacterial genetics has a significant role in determining pathogenicity, even after basic host
322 factors (age and sex) have been accounted for. An important limitation of our study is that we
323 did not use available information on host co-morbidities in BSI patients for the comparison
324 with commensal strains. In fact, the most frequent co-morbidity in the BSI collection is
325 immunosuppression, which was an exclusion criterion for the commensal collection. Co-
326 morbidities are associated with BSI (5, 18, 22). It is possible that co-morbidities act as a
327 confounder in our study, if they both increase the probability of BSI and influence the *E. coli*
328 strains carried by individuals. If this is the case, the variants we identify may not be directly
329 causal for infections. Rather, they may be bacterial variants that favor the colonization of
330 individuals with co-morbidities. Age is also associated with BSI (5, 14, 50). In this work, we
331 do control for age, albeit in a crude way, with the covariate “above or below 60 years old”. If
332 some of the variation associated with age is not captured by this covariate, some of the
333 variants we identify could favor the colonization of older or younger individuals. For
334 example, there is evidence of age-associated variants in *Streptococcus pneumoniae* (51). To
335 attenuate these concerns on confounding, we remind that several of the significant variants
336 have an experimentally validated role in infection and virulence (**Table 1**).

337 We found that strains from infections are more likely to be resistant to antimicrobials. What is
338 the mechanism behind this association, also found in similar GWAS conducted on other
339 pathogens (52, 53)? Confounding is a first possibility: hosts with co-morbidities are more
340 likely to develop a BSI and to use antibiotics frequently. Individuals may even be already
341 treated by antibiotics at the time of infection, in which case only resistant strains would be
342 able to cause this infection. If this mechanism operates, we could expect resistance to be more
343 frequent in hospital-associated than in community-associated BSI, if hosts in hospitals are

344 more likely to use antibiotics at the time of infection. However, we did not find any difference
345 between resistance in hospital-associated and community-associated BSI. Second,
346 antimicrobial resistance genes may have a causal role in infection. This seems unlikely given
347 their very specific function. Third, there might be a genetic association (linkage
348 disequilibrium) between resistance genes and genetic determinants of infection (52, 54). In
349 the third case, we expect the association to disappear when controlling for population
350 structure. With this control, we find that indeed, only one out of nine categories of resistance
351 is significantly enriched in BSI compared to commensals. This suggests that antibiotic
352 resistance genes are genetically linked with pathogenicity determinants, and opens the
353 interesting possibility that antibiotic resistance coevolves with pathogenicity determinants
354 associated with the clonal background of *E. coli*.

355 The present study compares *E. coli* whole genomes in colonization and in infection, as done
356 before for *Klebsiella pneumoniae* (52), *S. pneumoniae* (55), *Staphylococcus aureus* (53, 56),
357 *Neisseria meningitidis* (57). These GWAS studies presented a range of results, from low
358 heritability (2.6% for *S. aureus* carriage vs. BSI (53)), to intermediate (36.5% for *N.*
359 *meningitidis* carriage vs. invasive meningococcal disease), and an analogously large
360 heritability of 70% for *S. pneumoniae* invasive disease vs. carriage, along with a handful of
361 significant SNPs (55). We find a large heritability for *E. coli* BSI vs. colonization, which
362 suggests that a vaccine targeted at virulence determinants could reduce (at least temporarily)
363 the burden of infection (24).

364 The large heritability of *E. coli* capacity to cause infection also implies that this trait can
365 readily evolve. Evolution of *E. coli* pathogenicity would have important public health
366 implications, given that *E. coli* BSI are a major cause of morbidity and death in Western
367 countries. To investigate temporal trends in pathogenicity, we computed the pathogenicity
368 score with the machine learning model (used to predict the commensal vs. BSI status of
369 strains), in a dataset of commensals from 1980 to 2010 in France (18). We found that the
370 proportion of commensal *E. coli* isolates predicted to be pathogenic isolates with our trained
371 model increased over time, from 23% in the collection from 1980 to 46% in the collection
372 from 2010 (Figure S4). Applying this predictive model to the large collection of available *E.*
373 *coli* genome sequences, which currently numbers to more than 200,000 genomes (58), could
374 unravel the dynamics of pathogenicity across time and space. This effort would however need

375 to be properly controlled for the biases in the isolates sampled and sequenced (most of them
376 coming from infections), and the phylogroup-specific performance of the model.

377 What selective pressures might act on pathogenicity determinants? The capacity to cause
378 infection may not be selected *per se*, as infections are a relatively rare occurrence in the life
379 cycle of *E. coli* and do not obviously confer a transmission advantage. Pathogenicity
380 determinants have diverse functions and may therefore be selected for a variety of reasons.
381 They may for example improve the ability to colonize the human gut, improve the ability to
382 compete and replace existing strains, or allow longer persistence in the gut (59–62).
383 Elucidating the selective pressures acting on these determinants is an important research
384 question that would improve our understanding of *E. coli* pathogenicity.

385 This work opens perspectives to improve studies of the determinants of *E. coli* pathogenicity.
386 It remains difficult to pinpoint individual variants because of the clonal structure of *E. coli*,
387 and confounding by host factors is a concern. One idea to alleviate clonal structure is to focus
388 on specific STs. This would limit the dominant effect of STs belonging to phylogroup B2 and
389 carrying many virulence genes. However, the genetic diversity within a single ST might also
390 be limited. This makes it difficult to anticipate the results of such ST-focused studies. Another
391 idea is to extend to whole genomes the line of work comparing strains from infections vs.
392 colonization in the same individuals. This design would block host effects but, as stated in the
393 introduction, implies that power is contingent on the within-host diversity of strains present in
394 colonization. Further help will also likely come from linking pathogen diversity to clinical
395 and epidemiological phenotypes and including the genetic variation of the host into the
396 association such as in a previous study of *S. pneumoniae* (55). Lastly, similar studies should
397 be conducted in low and middle income countries, where a potentially very distinct diversity
398 of *E. coli* circulates (11) and where the public health problem posed by BSI will escalate with
399 the ageing population in the years to come.

400 In conclusion, we elucidated the bacterial genetic determinants of pathogenicity of the major
401 human pathogen *E. coli*. The capacity to cause BSI, particularly with urinary PE, is strongly
402 determined by sequence types, additional genetic factors, and tens of specific variants. This
403 implies that *E. coli* pathogenicity may evolve, informs future studies of *E. coli* mechanisms of

404 pathogenicity, and opens the possibility to reduce the burden of *E. coli* with a vaccine targeted
405 at these variants.

406 Material and methods

407 Strain collections

408 We studied the whole genomes of 1282 *E. coli* strains divided in two datasets, 370
409 commensals strains and 912 BSI strains. Commensal strains were gathered from stools of 370
410 healthy adults living in the Paris area or Brittany (both locations in the North of France)
411 between 2000 to 2017. These strains come from five previously published collections: ROAR
412 in 2000 (n=50)(63) (Brittany), LBC in 2001 (n=27)(64) (Brittany), PAR in 2002 (n=27)(64)
413 (Paris area), Coliville in 2010 (n=246)(65) (Paris area) and CEREMI in 2017 (n=20)(66)
414 (Paris area) (**Table S5**). In addition, a collection of 53 commensal strains from 53 healthy
415 subjects in Paris (37) was used to assess the temporal trend of pathogenicity. BSI isolates
416 (Colibafi (n=367) and Septicoli (n=545) collections) were collected at years 2005 and 2016-
417 2017, respectively (67). In all studies, one single *E. coli* colony randomly picked was retained
418 per individual after plating the blood cultures or the stools.

419 All multicenter clinical trials were approved by the appropriate ethic committees. The
420 Colibafi study was approved by the French Comité de Protection des Personnes of Hôpital
421 Saint-Louis, Paris, France (approval #2004-06, June 2004). The Septicoli study was approved
422 by the French Comité de Protection des Personnes Ile de France n°IV (IRB 00003835, March
423 2016). Because of their non-interventional nature, only an oral consent from patients was
424 requested under French Law. The study on the commensal strains was approved by the ethics
425 evaluation committee of Institut National de la Santé et de la Recherche Médicale (INSERM)
426 (CCTIRS no. 09.243, CNIL no. 909277, and CQI no. 01-014).

427 All the sequences were available (Bioproject PRJEB38489 (ROAR), PRJEB44819 (LBC),
428 PRJEB44872 (PAR), PRJEB39252 (Coliville), PRJEB39260 (Colibafi) and PRJEB35745
429 (Septicoli)) except the 20 samples of the CEREMI collection that were whole-genome
430 sequenced in the present work, following the protocol detailed in (21) (Bioproject
431 PRJEB55584).

432 **Genomic diversity of the core genome**

433 The 1282 assemblies were annotated with Prokka v1.14.6 (68). We then performed pan-
434 genome analysis from annotated assemblies with Panaroo v1.3.0 with strict clean mode and
435 the removal of invalid genes (69). We generated a core genome alignment spanning the whole
436 set of core genes as determined by Panaroo, and a phylogenetic tree was computed using
437 FastTree v2.1.11 (70).

438 **Comparison of commensal and BSI *E. coli* collection**

439 Multilocus sequence typing (MLST) was performed using an in-house script Petanc, that
440 integrates several existing bacterial genomic tools (71). We determined STs (Warwick MLST
441 scheme) (72) and O types (73).

442 We evaluated the risk of infection associated to colonization by a specific ST and by a
443 specific O-group. We compared the ST and O-group diversity from the collection of 912 BSI
444 isolates with the 370 commensal isolates, for all STs with at least 5 strains in at least one of
445 the two collections and for all O-groups with at least 5 strains in at least one of the two
446 collections.

447 The odds ratios for the infection risk were computed by fitting a logistic model of infection
448 status (commensal or BSI) as a function of the ST or the O-group (here and thereafter,
449 “significant” refers to significance at the 0.05 level).

450 Next, we compared the phylogenetic distribution of the commensal collection with the BSI
451 collection. For all strains, we calculated the cumulative frequency distribution of STs in the
452 commensal collection, and we compared it to the same distribution in 200 random sub-
453 samples of 370 sequences from the BSI collection.

454 We plotted the pangenome variation with the number of genomes analyzed (Panaroo output).
455 We evaluated the pangenome variation between commensal and BSI isolates with Panstripe
456 (74) using the output of FastTree (phylogeny of all strains) and Panaroo (gene presence
457 absence matrix). We randomly subsampled 100 trees of 370 tips from the BSI phylogeny
458 (n=912) and compared the rate of gene gain and loss between those trees and the commensal
459 tree (n=370). To quantify the genetic diversity, we computed the pairwise nucleotide diversity
460 (π)(75) in R (package ape)(76).

461 We also compared the number of virulence factors and the proportion of resistance strains
462 between commensal and BSI isolates. We performed t-tests to compare the distribution of
463 VAGs for each of the six main functional classes (adhesin, invasin, iron acquisition,
464 miscellaneous, protectin and toxin) and reported effect sizes using Cohen's d. Next, we
465 performed Fisher's exact tests to compare the proportions of strains carrying each VAG of a
466 given functional class between commensal and BSI isolates. All p-values were corrected for
467 multiple comparisons with the Benjamini-Hochberg method, with a 5% family-wise error
468 rate.

469 We predicted phenotypic resistance as described in (67) for nine antibiotics of clinical
470 importance (amikacin, ampicillin, carbapenem, cefotaxime/ceftazidime, cefepime,
471 fluoroquinolones, gentamicin, cotrimoxazole and piperacillin/tazobactam). We compared the
472 distribution of strains predicted to be resistant on each of the nine antibiotics using Fisher's
473 exact tests. We again corrected the p-values for multiple tests with the Benjamini-Hochberg
474 method.

475 [Heritability estimates](#)

476 We estimated narrow-sense heritability for the target variable using 2 different covariance
477 matrices: one built from the phylogroup using a kinship matrix, and another one with the age.
478 Limix v3.04 (77) was used, assuming normal errors for the point estimate.

479 [Association analysis](#)

480 We derived unitigs using unitig-counter v1.1.0 (78). We tested locus effects using the wg
481 (whole genome) model of pyseer v1.3.6 (29, 79), which trains a linear model with elastic net
482 regularization using the presence/absence patterns of all unitigs. We used an alpha with value
483 of 1 for the elastic net, which is equivalent to a lasso model. Cross-validation was performed
484 by holding out each phylogroup sequentially. The model performance was assessed by
485 computing three metrics using each phylogroup. The precision, as the measure of how many
486 positive predictions made are correct; the recall, as the measure of how many positive cases
487 the classifier predicted correctly over all the positive cases; and the F1-score, as the harmonic
488 mean of the two metrics. The F1-score expected by chance was computed overall, for each
489 phylogroup and for the different subsets, by randomly assigning the phenotype to the test
490 samples and running 1000 randomizations. The unitigs with a non-zero model coefficient

491 were mapped back to all input genomes, and gene families were annotated by taking a
492 representative protein sequence from all genomes encoding each gene, which was then used
493 as the input for eggNOG-mapper v2.1.3 using the panaroo output to collapse gene hits to
494 individual groups of orthologs. GO terms enrichment was determined using goatools v1.2.3
495 (80). An *in-house* list of *E. coli* virulence genes and antibiotic resistance genes was used to
496 annotate the virulence and antibiotic resistant genes within the collection, and a Fisher's exact
497 test was used to determine the enriched genes, with a multiple testing correction based on the
498 Benjamini-Hochberg method, with a 5% family-wise error rate. For the COG and virulence
499 genes enrichment analysis a random ST131 genome from the full dataset was picked up as
500 background.

501 [Prediction analysis](#)

502 We used unitig-caller v1.3.0 (81) to make variant calls in the test population, and the elastic
503 net regularization, previously trained, model using pyseer v1.3.6 (79) to predict the phenotype
504 in new commensal samples from different time periods, divided in decades.

505 [Code availability](#)

506 Apart from the software packages mentioned in the previous sections, the following were
507 used to run the analysis and generate the visualizations presented in this work: pandas v1.3.4
508 (82), numpy v1.20.3 (82), scipy v1.7.1 (83), matplotlib v3.4.3 (84), seaborn v0.11.2 (85),
509 biopython v1.80 (86) jupyterlab v3.2.1 (87). Most of the analysis were incorporated in a
510 reproducible pipeline using snakemake v7.18.1 (88) and conda v4.10.3 (89), which is
511 available as a code repository on GitHub
512 (https://github.com/jburgaya/2022_ecoli_commensal) under a permissive licence (MIT).

513 Acknowledgments

514 ED was partially supported by the “Fondation pour la Recherche Médicale” (Equipe FRM
515 2016, grant number DEQ20161136698). GR was supported by a “Poste d'accueil” funded by
516 the “Assistance Publique-Hôpitaux de Paris” (AP-HP) and the “Commissariat à l'énergie
517 atomique et aux énergies alternatives” (CEA) personal grant for his PhD. MG and JB were
518 supported by the Deutsche Forschungsgemeinschaft (DFG, German Research Foundation)
519 under Germany's Excellence Strategy - EXC 2155 - project number 390874280. JB was
520 further supported by the Deutsche Forschungsgemeinschaft grant number GA 3191/1-1.

521 The Colibafi/Septicoli group is composed of: Michel Wolff, Loubna Alavoine, Xavier Duval,
522 David Skurnik, Paul-Louis Woerther, Antoine Andremont, Etienne Carbonnelle, Olivier
523 Lortholary, Xavier Nassif, Sophie Abgrall, Françoise Jaureguy, Bertrand Picard, Véronique
524 Houdouin, Yannick Aujard, Stéphane Bonacorsi, Agnès Meybeck, Guilène Barnaud,
525 Catherine Branger, Agnès Lefort, Bruno Fantin, Claire Bellier, Frédéric Bert, Marie-Hélène
526 Nicolas-Chanoine, Bernard Page, Julie Cremniter, Jean-Louis Gaillard, Françoise Leturdu,
527 Jean-Pierre Sollet, Gaëtan Plantefève, Xavière Panhard, France Mentré, Estelle Marcault,
528 Florence Tubach, Virginie Zarrouk, Frederic Bert, Marion Duprilot, Véronique Leflon-
529 Guibout, Naouale Maataoui, Laurence Armand, Liem Luong Nguyen, Rocco Collarino,
530 Anne-Lise Munier, Hervé Jacquier, Emmanuel Lecorché, Laetitia Coutte, Camille Gomart,
531 Ousser Ahmed Fateh, Luce Landraud, Jonathan Messika, Elisabeth Aslangul, Magdalena
532 Gerin, Alexandre Bleibtreu, Mathilde Lescat, Violaine Walewski, Frederic Mechaï, Marion
533 Dollat, Anne-Claire Maherault, Mélanie Mercier-Darty, Bernadette Basse, Bruno Fantin,
534 Xavier Duval, Etienne Carbonnelle, Jean-Winoc Decousser, Raphaël Lepeule.

535 The COLIVILLE group is composed of: Monique Allouche, Jean-Pierre Aubert, Isabelle
536 Aubin, Ghislaine Audran, Dan Baruch, Philippe Birembaux, Max Budowski, Emilie Chemla,
537 Alain Eddi, Marc Frarier, Eric Galam, Julien Gelly, Serge Joly, Jean-François Millet, Michel
538 Nougairede, Nadja Pillon, Guy Septavaux, Catherine Szwebel, Philippe Vellard, Raymond
539 Wakim, Xavier Watelet and Philippe Zerr.

540 Bibliography

541 1. Goto M, McDanel JS, Jones MM, Livorsi DJ, Ohl ME, Beck BF, Richardson KK,
542 Alexander B, Perencevich EN. 2017. Antimicrobial Nonsusceptibility of Gram-Negative
543 Bloodstream Isolates, Veterans Health Administration System, United States, 2003–20131.
544 Emerg Infect Dis 23:1815–1825.

545 2. Kraker MEA de, Davey PG, Grundmann H, Group on behalf of the B study. 2011.
546 Mortality and Hospital Stay Associated with Resistant *Staphylococcus aureus* and *Escherichia*
547 *coli* Bacteremia: Estimating the Burden of Antibiotic Resistance in Europe. PLOS Medicine
548 8:e1001104.

549 3. Abernethy JK, Johnson AP, Guy R, Hinton N, Sheridan EA, Hope RJ. 2015. Thirty day
550 all-cause mortality in patients with *Escherichia coli* bacteraemia in England. Clinical
551 Microbiology and Infection 21:251.e1-251.e8.

552 4. Feldman SF, Temkin E, Wullhart L, Nutman A, Schechner V, Shitrit P, Shvartz R,
553 Schwaber MJ, Andremont A, Carmeli Y. 2022. A nationwide population-based study of
554 *Escherichia coli* bloodstream infections: incidence, antimicrobial resistance and mortality.
555 Clinical Microbiology and Infection 28:879.e1-879.e7.

556 5. Bonten M, Johnson JR, van den Biggelaar AHJ, Georgalis L, Geurtsen J, de Palacios PI,
557 Gravenstein S, Verstraeten T, Hermans P, Poolman JT. 2021. Epidemiology of *Escherichia*
558 *coli* Bacteremia: A Systematic Literature Review. Clinical Infectious Diseases 72:1211–1219.

559 6. Gladstone RA, McNally A, Pöntinen AK, Tonkin-Hill G, Lees JA, Skytén K, Cléon F,
560 Christensen MOK, Haldorsen BC, Bye KK, Gammelsrud KW, Hjetland R, Kümmel A,
561 Larsen HE, Lindemann PC, Löhr IH, Marvik Å, Nilsen E, Noer MT, Simonsen GS, Steinbakk
562 M, Tofteland S, Vattøy M, Bentley SD, Croucher NJ, Parkhill J, Johnsen PJ, Samuelsen Ø,
563 Corander J. 2020. Emergence and Dissemination of Antimicrobial Resistance in *Escherichia*
564 *Coli* Causing Bloodstream Infections: A Nationwide Longitudinal Microbial Population
565 Genomic Cohort Study in Norway between 2002-2017. 3645193. SSRN Scholarly Paper.
566 Rochester, NY <https://doi.org/10.2139/ssrn.3645193>.

567 7. Kallonen T, Brodrick HJ, Harris SR, Corander J, Brown NM, Martin V, Peacock SJ,
568 Parkhill J. 2017. Systematic longitudinal survey of invasive *Escherichia coli* in England
569 demonstrates a stable population structure only transiently disturbed by the emergence of
570 ST131. *Genome research* 27:1437–1449.

571 8. Petty NK, Zakour NLB, Stanton-Cook M, Skippington E, Totsika M, Forde BM, Phan M-
572 D, Moriel DG, Peters KM, Davies M, Beatson SA. 2014. Global dissemination of a multidrug
573 resistant *Escherichia coli* clone. *Proceedings of the National Academy of Sciences* 111:5694–
574 5699.

575 9. Nicolas-Chanoine M-H, Bertrand X, Madec J-Y. 2014. *Escherichia coli* ST131, an
576 intriguing Clonal Group. *Clinical Microbiology Reviews* 27:543–574.

577 10. Casadevall A, Pirofski LA. 1999. Host-pathogen interactions: redefining the basic
578 concepts of virulence and pathogenicity. *Infect Immun* 67:3703–3713.

579 11. Tenaillon O, Skurnik D, Picard B, Denamur E. 2010. The population genetics of
580 commensal *Escherichia coli*. *Nature Reviews Microbiology* 8:207.

581 12. Kang C-I, Song J-H, Chung DR, Peck KR, Ko KS, Yeom J-S, Ki HK, Son JS, Lee SS,
582 Kim Y-S, Jung S-I, Kim S-W, Chang H-H, Ryu SY, Kwon KT, Lee H, Moon C, Shin SY.
583 2010. Risk factors and treatment outcomes of community-onset bacteraemia caused by
584 extended-spectrum β -lactamase-producing *Escherichia coli*. *International Journal of*
585 *Antimicrobial Agents* 36:284–287.

586 13. Blandy O, Honeyford K, Gharbi M, Thomas A, Ramzan F, Ellington MJ, Hope R,
587 Holmes AH, Johnson AP, Aylin P, Woodford N, Sriskandan S. 2019. Factors that impact on
588 the burden of *Escherichia coli* bacteraemia: multivariable regression analysis of 2011–2015
589 data from West London. *Journal of Hospital Infection* 101:120–128.

590 14. Laupland KB, Gregson DB, Church DL, Ross T, Pitout JDD. 2008. Incidence, risk
591 factors and outcomes of *Escherichia coli* bloodstream infections in a large Canadian region.
592 *Clinical Microbiology and Infection* 14:1041–1047.

593 15. Galardini M, Clermont O, Baron A, Busby B, Dion S, Schubert S, Beltrao P, Denamur
594 E. 2020. Major role of iron uptake systems in the intrinsic extra-intestinal virulence of the

595 genus *Escherichia* revealed by a genome-wide association study. PLOS Genetics
596 16:e1009065.

597 16. Johnson JR. 1991. Virulence factors in *Escherichia coli* urinary tract infection. Clinical
598 Microbiology Reviews 4:80–128.

599 17. Clermont O, Couffignal C, Blanco J, Mentré F, Picard B, Denamur E, Groups the C
600 and C. 2017. Two levels of specialization in bacteraemic *Escherichia coli* strains revealed by
601 their comparison with commensal strains. Epidemiology & Infection 145:872–882.

602 18. Marin J, Clermont O, Royer G, Mercier-Darty M, Decousser JW, Tenaillon O,
603 Denamur E, Blanquart F. 2022. The Population Genomics of Increased Virulence and
604 Antibiotic Resistance in Human Commensal *Escherichia coli* over 30 Years in France.
605 Applied and Environmental Microbiology 0:e00664-22.

606 19. Lefort A, Panhard X, Clermont O, Woerther P-L, Branger C, Mentré F, Fantin B,
607 Wolff M, Denamur E. 2011. Host Factors and Portal of Entry Outweigh Bacterial
608 Determinants To Predict the Severity of *Escherichia coli* Bacteremia. Journal of Clinical
609 Microbiology 49:777–783.

610 20. Salipante SJ, Roach DJ, Kitzman JO, Snyder MW, Stackhouse B, Butler-Wu SM, Lee
611 C, Cookson BT, Shendure J. 2015. Large-scale genomic sequencing of extraintestinal
612 pathogenic *Escherichia coli* strains. Genome Research 25:119–128.

613 21. de Lastours V, Laouénan C, Royer G, Carbonnelle E, Lepeule R, Esposito-Farèse M,
614 Clermont O, Duval X, Fantin B, Mentré F, Decousser JW, Denamur E, Lefort A. 2020.
615 Mortality in *Escherichia coli* bloodstream infections: antibiotic resistance still does not make
616 it. J Antimicrob Chemother 75:2334–2343.

617 22. Denamur E, Condamine B, Esposito-Farèse M, Royer G, Clermont O, Laouenan C,
618 Lefort A, Lastours V de, Galardini M, Colibafi T, Groups S. 2022. Genome wide association
619 study of *Escherichia coli* bloodstream infection isolates identifies genetic determinants for the
620 portal of entry but not fatal outcome. PLOS Genetics 18:e1010112.

621 23. Horesh G, Taylor-Brown A, McGimpsey S, Lassalle F, Corander J, Heinz E, Thomson
622 NRY 2021. Different evolutionary trends form the twilight zone of the bacterial pan-genome.
623 Microbial Genomics 7:000670.

624 24. Frenck RW, Ervin J, Chu L, Abbanat D, Spiessens B, Go O, Haazen W, van den
625 Dobbelsteen G, Poolman J, Thoelen S, Ibarra de Palacios P. 2019. Safety and immunogenicity
626 of a vaccine for extra-intestinal pathogenic *Escherichia coli* (ESTELLA): a phase 2
627 randomised controlled trial. *The Lancet Infectious Diseases* 19:631–640.

628 25. Huttner A, Hatz C, van den Dobbelsteen G, Abbanat D, Hornacek A, Frölich R,
629 Dreyer AM, Martin P, Davies T, Fae K, van den Nieuwenhof I, Thoelen S, de Vallière S,
630 Kuhn A, Bernasconi E, Viereck V, Kavvadias T, Kling K, Ryu G, Hülder T, Gröger S,
631 Scheiner D, Alaimo C, Harbarth S, Poolman J, Fonck VG. 2017. Safety, immunogenicity, and
632 preliminary clinical efficacy of a vaccine against extraintestinal pathogenic *Escherichia coli* in
633 women with a history of recurrent urinary tract infection: a randomised, single-blind, placebo-
634 controlled phase 1b trial. *The Lancet Infectious Diseases* 17:528–537.

635 26. Lane MC, Mobley HLT. 2007. Role of P-fimbrial-mediated adherence in
636 pyelonephritis and persistence of uropathogenic *Escherichia coli* (UPEC) in the mammalian
637 kidney. *Kidney International* 72:19–25.

638 27. Snyder JA, Lloyd AL, Lockatell CV, Johnson DE, Mobley HLT. 2006. Role of Phase
639 Variation of Type 1 Fimbriae in a Uropathogenic *Escherichia coli* Cystitis Isolate during
640 Urinary Tract Infection. *Infection and Immunity* 74:1387–1393.

641 28. Visscher PM, Hill WG, Wray NR. 2008. Heritability in the genomics era: concepts and
642 misconceptions. *Nature Reviews Genetics* 9:255–266.

643 29. Lees JA, Mai TT, Galardini M, Wheeler NE, Horsfield ST, Parkhill J, Corander J.
644 2020. Improved Prediction of Bacterial Genotype-Phenotype Associations Using Interpretable
645 Pangenome-Spanning Regressions. *mBio* 11:e01344-20.

646 30. de Lorenzo V, Bindereif A, Paw BH, Neilands JB. 1986. Aerobactin biosynthesis and
647 transport genes of plasmid ColV-K30 in *Escherichia coli* K-12. *J Bacteriol* 165:570–578.

648 31. Hultgren SJ, Lindberg F, Magnusson G, Kihlberg J, Tennent JM, Normark S. 1989.
649 The PapG adhesin of uropathogenic *Escherichia coli* contains separate regions for receptor
650 binding and for the incorporation into the pilus. *Proceedings of the National Academy of
651 Sciences* 86:4357–4361.

652 32. Biggel M, Xavier BB, Johnson JR, Nielsen KL, Frimodt-Møller N, Matheeussen V,
653 Goossens H, Moons P, Van Puyvelde S. 2020. Horizontally acquired papGII-containing
654 pathogenicity islands underlie the emergence of invasive uropathogenic *Escherichia coli*
655 lineages. *1. Nat Commun* 11:5968.

656 33. Norris FA, Wilson MP, Wallis TS, Galyov EE, Majerus PW. 1998. SopB, a protein
657 required for virulence of *Salmonella dublin*, is an inositol phosphate phosphatase. *Proc Natl
658 Acad Sci U S A* 95:14057–14059.

659 34. Crépin S, Ottosen EN, Peters K, Smith SN, Himpel SD, Vollmer W, Mobley HLT.
660 2018. The lytic transglycosylase MltB connects membrane homeostasis and in vivo fitness of
661 *Acinetobacter baumannii*. *Mol Microbiol* 109:745–762.

662 35. Raha M, Sockett H, Macnab RM. 1994. Characterization of the fliL gene in the
663 flagellar regulon of *Escherichia coli* and *Salmonella typhimurium*. *J Bacteriol* 176:2308–
664 2311.

665 36. Bindal G, Krishnamurthi R, Seshasayee ASN, Rath D. 2017. CRISPR-Cas-Mediated
666 Gene Silencing Reveals RacR To Be a Negative Regulator of YdaS and YdaT Toxins in
667 *Escherichia coli* K-12. *mSphere* 2:e00483-17.

668 37. Duriez P, Clermont O, Bonacorsi S, Bingen E, Chaventé A, Elion J, Picard B,
669 Denamur E 2001. Commensal *Escherichia coli* isolates are phylogenetically distributed
670 among geographically distinct human populations. *Microbiology* 147:1671–1676.

671 38. Artola-Recolons C, Lee M, Bernardo-García N, Blázquez B, Hesek D, Bartual SG,
672 Mahasenan KV, Lastochkin E, Pi H, Boggess B, Meindl K, Usón I, Fisher JF, Mobashery S,
673 Hermoso JA. 2014. Structure and Cell Wall Cleavage by Modular Lytic Transglycosylase
674 MltC of *Escherichia coli*. *ACS Chem Biol* 9:2058–2066.

675 39. Li B, Huang Q, Cui A, Liu X, Hou B, Zhang L, Liu M, Meng X, Li S. 2018.
676 Overexpression of Outer Membrane Protein X (OmpX) Compensates for the Effect of TolC
677 Inactivation on Biofilm Formation and Curli Production in Extraintestinal Pathogenic
678 *Escherichia coli* (ExPEC). *Frontiers in Cellular and Infection Microbiology* 8.

679 40. Maynard C, Bekal S, Sanschagrin F, Levesque RC, Brousseau R, Masson L, Larivière
680 S, Harel J. 2004. Heterogeneity among Virulence and Antimicrobial Resistance Gene Profiles

681 of Extraintestinal *Escherichia coli* Isolates of Animal and Human Origin. *Journal of Clinical*
682 *Microbiology* 42:5444–5452.

683 41. Sampaio SCF, Luiz WB, Vieira MAM, Ferreira RCC, Garcia BG, Sinigaglia-Coimbra
684 R, Sampaio JLM, Ferreira LCS, Gomes TAT. 2016. Flagellar Cap Protein FliD Mediates
685 Adherence of Atypical Enteropathogenic *Escherichia coli* to Enterocyte Microvilli. *Infect*
686 *Immun* 84:1112–1122.

687 42. Pfiffer V, Sarenko O, Possling A, Hengge R. 2019. Genetic dissection of *Escherichia*
688 *coli*'s master diguanylate cyclase DgcE: Role of the N-terminal MASE1 domain and direct
689 signal input from a GTPase partner system. *PLOS Genetics* 15:e1008059.

690 43. Li H, Xia Y, Tian Z, Jin Y, Bai F, Cheng Z, Swietnicki W, Wu W, Pan X. 2022.
691 Dihydrolipoamide Acetyltransferase AceF Influences the Type III Secretion System and
692 Resistance to Oxidative Stresses through RsmY/Z in *Pseudomonas aeruginosa*.
693 *Microorganisms* 10:666.

694 44. Serfiotis-Mitsa D, Herbert AP, Roberts GA, Soares DC, White JH, Blakely GW, Uhrín
695 D, Dryden DTF. 2010. The structure of the KlcA and ArdB proteins reveals a novel fold and
696 antirestriction activity against Type I DNA restriction systems in vivo but not in vitro. *Nucleic*
697 *Acids Res* 38:1723–1737.

698 45. Ravan H, Amandadi M. 2015. Analysis of yeh Fimbrial Gene Cluster in *Escherichia*
699 *coli* O157:H7 in Order to Find a Genetic Marker for this Serotype. *Curr Microbiol* 71:274–
700 282.

701 46. Kauffman J. 1947. The Serology of the Coli Group. *The Journal of Immunology*
702 57:71–100.

703 47. Johnson JR, Johnston BD, Porter S, Thuras P, Aziz M, Price LB. 2019. Accessory
704 Traits and Phylogenetic Background Predict *Escherichia coli* Extraintestinal Virulence Better
705 Than Does Ecological Source. *J Infect Dis* 219:121–132.

706 48. Picard B, Garcia JS, Gouriou S, Duriez P, Brahimi N, Bingen E, Elion J, Denamur E.
707 1999. The link between phylogeny and virulence in *Escherichia coli* extraintestinal infection?
708 *Infection and Immunity* 67:546–553.

709 49. Johnson JR, Kuskowski M. 2000. Clonal Origin, Virulence Factors, and Virulence.
710 Infect Immun 68:424–425.

711 50. Roubaud Baudron C, Panhard X, Clermont O, Mentré F, Fantin B, Denamur E, Lefort
712 A, COLIBAFI Group. 2014. *Escherichia coli* bacteraemia in adults: age-related differences in
713 clinical and bacteriological characteristics, and outcome. Epidemiol Infect 142:2672–2683.

714 51. Kremer PHC, Ferwerda B, Bootsma HJ, Rots NY, Wijmenga-Monsuur AJ, Sanders
715 EAM, Trzciński K, Wyllie AL, Turner P, van der Ende A, Brouwer MC, Bentley SD, van de
716 Beek D, Lees JA. 2022. Pneumococcal genetic variability in age-dependent bacterial carriage.
717 Elife 11:e69244.

718 52. Vornhagen J, Roberts EK, Unverdorben L, Mason S, Patel A, Crawford R, Holmes
719 CL, Sun Y, Teodorescu A, Snitkin ES, Zhao L, Simner PJ, Tamma PD, Rao K, Kaye KS,
720 Bachman MA. 2022. Combined comparative genomics and clinical modeling reveals
721 plasmid-encoded genes are independently associated with *Klebsiella* infection. Nat Commun
722 13:4459.

723 53. Young BC, Wu C-H, Charlesworth J, Earle S, Price JR, Gordon NC, Cole K, Dunn L,
724 Liu E, Oakley S, Godwin H, Fung R, Miller R, Knox K, Votintseva A, Quan TP, Tilley R,
725 Scarborough M, Crook DW, Peto TE, Walker AS, Llewelyn MJ, Wilson DJ. 2021.
726 Antimicrobial resistance determinants are associated with *Staphylococcus aureus* bacteraemia
727 and adaptation to the healthcare environment: a bacterial genome-wide association study.
728 Microb Genom 7.

729 54. Biggel M, Moons P, Nguyen MN, Goossens H, Van Puyvelde S. 2022. Convergence
730 of virulence and antimicrobial resistance in increasingly prevalent *Escherichia coli* ST131
731 papGII+ sublineages. Commun Biol 5:752.

732 55. Lees JA, Ferwerda B, Kremer PHC, Wheeler NE, Serón MV, Croucher NJ, Gladstone
733 RA, Bootsma HJ, Rots NY, Wijmenga-Monsuur AJ, Sanders EAM, Trzciński K, Wyllie AL,
734 Zwinderman AH, van den Berg LH, van Rheenen W, Veldink JH, Harboe ZB, Lundbo LF, de
735 Groot LCPGM, van Schoor NM, van der Velde N, Ängquist LH, Sørensen TIA, Nohr EA,
736 Mentzer AJ, Mills TC, Knight JC, du Plessis M, Nzenze S, Weiser JN, Parkhill J, Madhi S,
737 Benfield T, von Gottberg A, van der Ende A, Brouwer MC, Barrett JC, Bentley SD, van de

738 Beek D. 2019. Joint sequencing of human and pathogen genomes reveals the genetics of
739 pneumococcal meningitis. *1. Nat Commun* 10:2176.

740 56. Young BC, Earle SG, Soeng S, Sar P, Kumar V, Hor S, Sar V, Bousfield R, Sanderson
741 ND, Barker L, Stoesser N, Emery KR, Parry CM, Nickerson EK, Turner P, Bowden R, Crook
742 DW, Wyllie DH, Day NP, Wilson DJ, Moore CE. 2019. Panton-Valentine leucocidin is the
743 key determinant of *Staphylococcus aureus* pyomyositis in a bacterial GWAS. *Elife* 8:e42486.

744 57. Earle SG, Lobanova M, Lavender H, Tang C, Exley RM, Ramos-Sevillano E,
745 Browning DF, Kostiou V, Harrison OB, Bratcher HB, Varani G, Tang CM, Wilson DJ,
746 Maiden MCJ. 2021. Genome-wide association studies reveal the role of polymorphisms
747 affecting factor H binding protein expression in host invasion by *Neisseria meningitidis*. *PLoS*
748 *Pathog* 17:e1009992.

749 58. Zhou Z, Alikhan N-F, Mohamed K, Fan Y, Achtman M. 2020. The Enterobase user's
750 guide, with case studies on *Salmonella* transmissions, *Yersinia pestis* phylogeny, and
751 *Escherichia* core genomic diversity. *Genome Res* 30:138–152.

752 59. Ostblom A, Adlerberth I, Wold AE, Nowrouzian FL. 2011. *Escherichia coli*
753 pathogenicity island-markers, *malX* and *usp* and the capacity to persist in the infant's
754 commensal microbiota. *Applied and environmental microbiology* 77:2303–2308.

755 60. Nowrouzian F, Hesselmar B, Saalman R, Strannegård IL, Åberg N, Wold AE,
756 Adlerberth I. 2003. *Escherichia coli* in infants' intestinal microflora: Colonization rate, strain
757 turnover, and virulence gene carriage. *Pediatric Research* 54:8–14.

758 61. Le Gall T, Clermont O, Gouriou S, Picard B, Nassif X, Denamur E, Tenaillon O.
759 2007. Extraintestinal virulence is a coincidental by-product of commensalism in b2
760 phylogenetic group *Escherichia coli* strains. *Molecular Biology and Evolution* 24:2373–2384.

761 62. Diard M, Garry L, Selva M, Mosser T, Denamur E, Matic I. 2010. Pathogenicity-
762 associated islands in extraintestinal pathogenic *Escherichia coli* are fitness elements involved
763 in intestinal colonization. *Journal of Bacteriology* 192:4885–4893.

764 63. Skurnik D, Clermont O, Guillard T, Launay A, Danilchanka O, Pons S, Diancourt L,
765 Lebreton F, Kadlec K, Roux D, Jiang D, Dion S, Aschard H, Denamur M, Cywes-Bentley C,
766 Schwarz S, Tenaillon O, Andremont A, Picard B, Mekalanos J, Brisson S, Denamur E. 2016.

767 Emergence of Antimicrobial-Resistant *Escherichia coli* of Animal Origin Spreading in
768 Humans. *Molecular Biology and Evolution* 33:898–914.

769 64. Escobar-Páramo P, Grenet K, Menac'h AL, Rode L, Salgado E, Amorin C, Gouriou S,
770 Picard B, Rahimy MC, Andremont A, Denamur E, Ruimy R. 2004. Large-Scale Population
771 Structure of Human Commensal *Escherichia coli* Isolates. *Appl Environ Microbiol* 70:5698–
772 5700.

773 65. Massot M, Daubié A-S, Clermont O, Jaureguy F, Couffignal C, Dahbi G, Mora A,
774 Blanco J, Branger C, Mentré F, Eddi A, Picard B, Denamur E. 2016. Phylogenetic, virulence
775 and antibiotic resistance characteristics of commensal strain populations of *Escherichia coli*
776 from community subjects in the Paris area in 2010 and evolution over 30 years. *Microbiology*
777 162:642–650.

778 66. Burdet C, Grall N, Linard M, Bridier-Nahmias A, Benhayoun M, Bourabha K,
779 Magnan M, Clermont O, d'Humières C, Tenaillon O, Denamur E, Massias L, Tubiana S,
780 Alavoine L, Andremont A, Mentré F, Duval X, for the CEREMI Group. 2019. Ceftriaxone
781 and Cefotaxime Have Similar Effects on the Intestinal Microbiota in Human Volunteers
782 Treated by Standard-Dose Regimens. *Antimicrobial Agents and Chemotherapy* 63:e02244-
783 18.

784 67. Royer G, Darty MM, Clermont O, Condamine B, Laouenan C, Decousser J-W,
785 Vallenet D, Lefort A, de Lastours V, Denamur E, Wolff M, Alavoine L, Duval X, Skurnik D,
786 Woerther P-L, Andremont A, Carbonnelle E, Lortholary O, Nassif X, Abgrall S, Jaureguy F,
787 Picard B, Houdouin V, Aujard Y, Bonacorsi S, Meybeck A, Barnaud G, Branger C, Lefort A,
788 Fantin B, Bellier C, Bert F, Nicolas-Chanoine M-H, Page B, Cremniter J, Gaillard J-L,
789 Leturdu F, Sollet J-P, Plantefève G, Panhard X, Mentré F, Marcault E, Tubach F, Zarrouk V,
790 Bert F, Duprilot M, Leflon-Guibout V, Maataoui N, Armand L, Nguyen LL, Collarino R,
791 Munier A-L, Jacquier H, Lecorché E, Coutte L, Gomart C, Fateh OA, Landraud L, Messika J,
792 Aslangul E, Gerin M, Bleibtreu A, Lescat M, Walewski V, Mechaï F, Dollat M, Maherault A-
793 C, Wolff M, Mercier-Darty M, Basse B, COLIBAFI and SEPTICOLI groups. 2021.
794 Phylogroup stability contrasts with high within sequence type complex dynamics of
795 *Escherichia coli* bloodstream infection isolates over a 12-year period. *Genome Med* 13:77.

796 68. Seemann T. 2014. Prokka: rapid prokaryotic genome annotation. *Bioinformatics*
797 30:2068–2069.

798 69. Tonkin-Hill G, MacAlasdair N, Ruis C, Weimann A, Horesh G, Lees JA, Gladstone
799 RA, Lo S, Beaudoin C, Floto RA, Frost SDW, Corander J, Bentley SD, Parkhill J. 2020.
800 Producing polished prokaryotic pangenomes with the Panaroo pipeline. *Genome Biology*
801 21:180.

802 70. Price MN, Dehal PS, Arkin AP. 2010. FastTree 2 – Approximately Maximum-
803 Likelihood Trees for Large Alignments. *PLOS ONE* 5:e9490.

804 71. Bourrel AS, Poirel L, Royer G, Darty M, Vuillemin X, Kieffer N, Clermont O,
805 Denamur E, Nordmann P, Decousser J-W, IAME Resistance Group. 2019. Colistin resistance
806 in Parisian inpatient faecal *Escherichia coli* as the result of two distinct evolutionary
807 pathways. *J Antimicrob Chemother* 74:1521–1530.

808 72. Wirth T, Falush D, Lan R, Colles F, Mensa P, Wieler LH, Karch H, Reeves PR,
809 Maiden MCJ, Ochman H, Achtman M. 2006. Sex and virulence in *Escherichia coli*: an
810 evolutionary perspective. *Mol Microbiol* 60:1136–1151.

811 73. Ingle DJ, Valcanis M, Kuzevski A, Tauschek M, Inouye M, Stinear T, Levine MM,
812 Robins-Browne RM, Holt KE. 2016. In silico serotyping of *E. coli* from short read data
813 identifies limited novel O-loci but extensive diversity of O:H serotype combinations within
814 and between pathogenic lineages. *Microb Genom* 2:e000064.

815 74. Tonkin-Hill G, Gladstone RA, Pöntinen AK, Arredondo-Alonso S, Bentley SD,
816 Corander J. 2022. Robust analysis of prokaryotic pangenome gene gain and loss rates with
817 Panstripe. *bioRxiv* <https://doi.org/10.1101/2022.04.23.489244>.

818 75. Nei M. 1987. *Molecular evolutionary genetics*. Columbia university press.

819 76. Paradis E, Schliep K. 2019. ape 5.0: an environment for modern phylogenetics and
820 evolutionary analyses in R. *Bioinformatics* 35:526–528.

821 77. Lippert C, Casale FP, Rakitsch B, Stegle O. 2014. LIMIX: genetic analysis of multiple
822 traits. *bioRxiv* <https://doi.org/10.1101/003905>.

823 78. Jaillard M, Lima L, Tournoud M, Mahé P, van Belkum A, Lacroix V, Jacob L. 2018.
824 A fast and agnostic method for bacterial genome-wide association studies: Bridging the gap
825 between k-mers and genetic events. *PLoS Genet* 14:e1007758.

826 79. Lees JA, Galardini M, Bentley SD, Weiser JN, Corander J. 2018. pyseer: a
827 comprehensive tool for microbial pangenome-wide association studies. *Bioinformatics*
828 34:4310–4312.

829 80. Klopfenstein DV, Zhang L, Pedersen BS, Ramírez F, Warwick Vesztrocy A, Naldi A,
830 Mungall CJ, Yunes JM, Botvinnik O, Weigel M, Dampier W, Dessimoz C, Flick P, Tang H.
831 2018. GOATOOLS: A Python library for Gene Ontology analyses. 1. *Sci Rep* 8:10872.

832 81. Holley G, Melsted P. 2020. Bifrost: highly parallel construction and indexing of
833 colored and compacted de Bruijn graphs. *Genome Biology* 21:249.

834 82. McKinney W. 2010. Data Structures for Statistical Computing in Python, p. 56–61.
835 *In* . Austin, Texas.

836 83. Virtanen P, Gommers R, Oliphant TE, Haberland M, Reddy T, Cournapeau D,
837 Burovski E, Peterson P, Weckesser W, Bright J, van der Walt SJ, Brett M, Wilson J, Millman
838 KJ, Mayorov N, Nelson ARJ, Jones E, Kern R, Larson E, Carey CJ, Polat İ, Feng Y, Moore
839 EW, VanderPlas J, Laxalde D, Perktold J, Cimrman R, Henriksen I, Quintero EA, Harris CR,
840 Archibald AM, Ribeiro AH, Pedregosa F, van Mulbregt P. 2020. SciPy 1.0: fundamental
841 algorithms for scientific computing in Python. 3. *Nat Methods* 17:261–272.

842 84. Hunter JD. 2007. Matplotlib: A 2D Graphics Environment. *Computing in Science and*
843 *Engg* 9:90–95.

844 85. Waskom M. 2021. seaborn: statistical data visualization. *JOSS* 6:3021.

845 86. Cock PJA, Antao T, Chang JT, Chapman BA, Cox CJ, Dalke A, Friedberg I,
846 Hamelryck T, Kauff F, Wilczynski B, de Hoon MJL. 2009. Biopython: freely available
847 Python tools for computational molecular biology and bioinformatics. *Bioinformatics*
848 25:1422–1423.

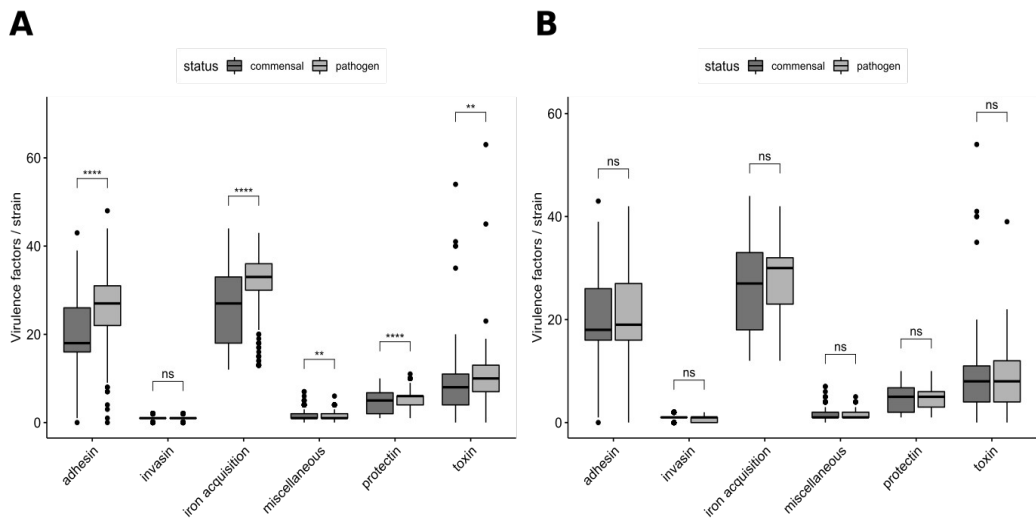
849 87. Kluyver T, Ragan-Kelley B, Pérez F, Bussonnier M, Frederic J, Hamrick J, Grout J,
850 Corlay S, Ivanov P, Abdalla S, Willing C. Jupyter Notebooks—a publishing format for
851 reproducible computational workflows.

852 88. Mölder F, Jablonski KP, Letcher B, Hall MB, Tomkins-Tinch CH, Sochat V, Forster J,
853 Lee S, Twardziok SO, Kanitz A, Wilm A, Holtgrewe M, Rahmann S, Nahnsen S, Köster J.
854 2021. Sustainable data analysis with Snakemake. *F1000Res* 10:33.

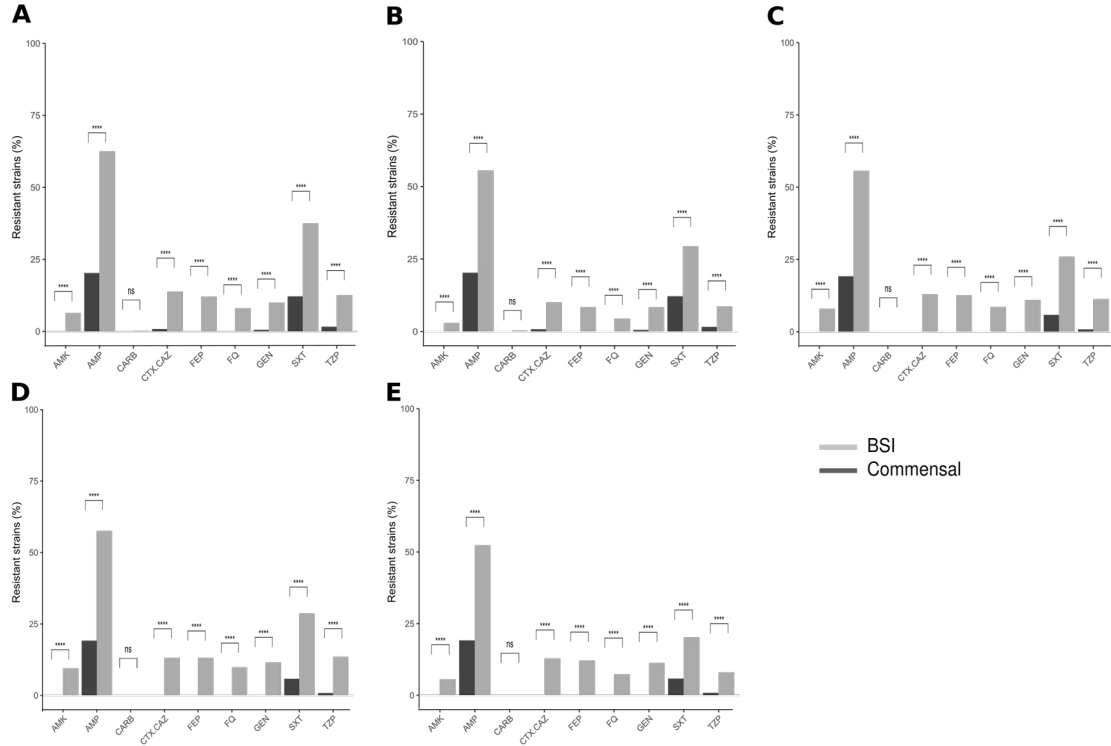
855 89. Grüning B, Dale R, Sjödin A, Chapman BA, Rowe J, Tomkins-Tinch CH, Valieris R,
856 Köster J. 2018. Bioconda: sustainable and comprehensive software distribution for the life
857 sciences. *7. Nat Methods* 15:475–476.

858

859 **Supplementary figures**

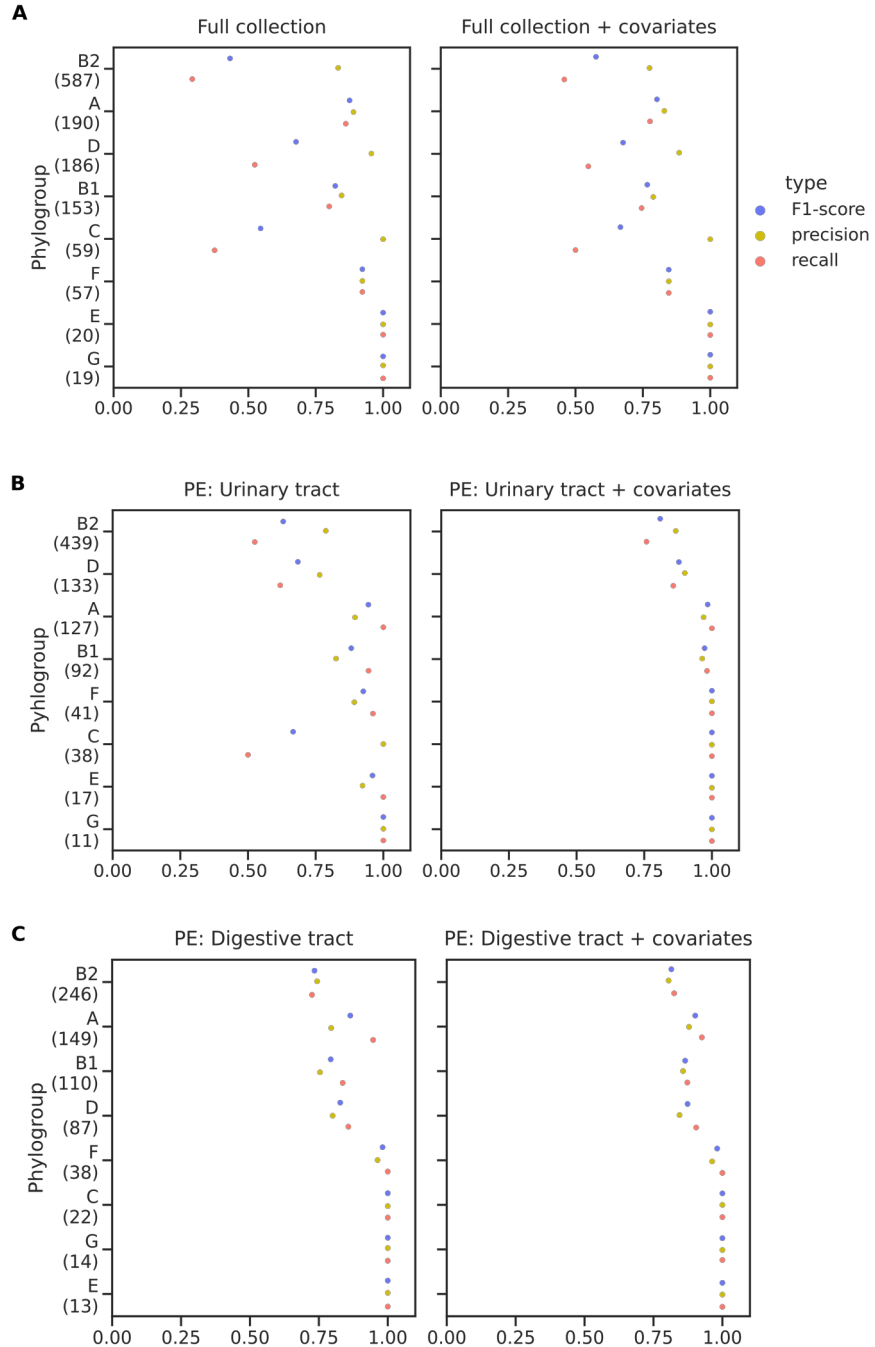


860 **Figure S1.** Distribution of the number of virulence factors per strain among the six main functional classes of
861 virulence (Benjamini-Hochberg corrected p value < 0.05) for (A) all the strains with a urinary portal of entry and
862 for (B) all the strains with a digestive portal of entry. Significant differences are indicated by asterisks (p value <
863 0.05: *; p value < 0.01: **; p value < 0.001: ***; p value < 0.0001: ****; ns: non-significant).

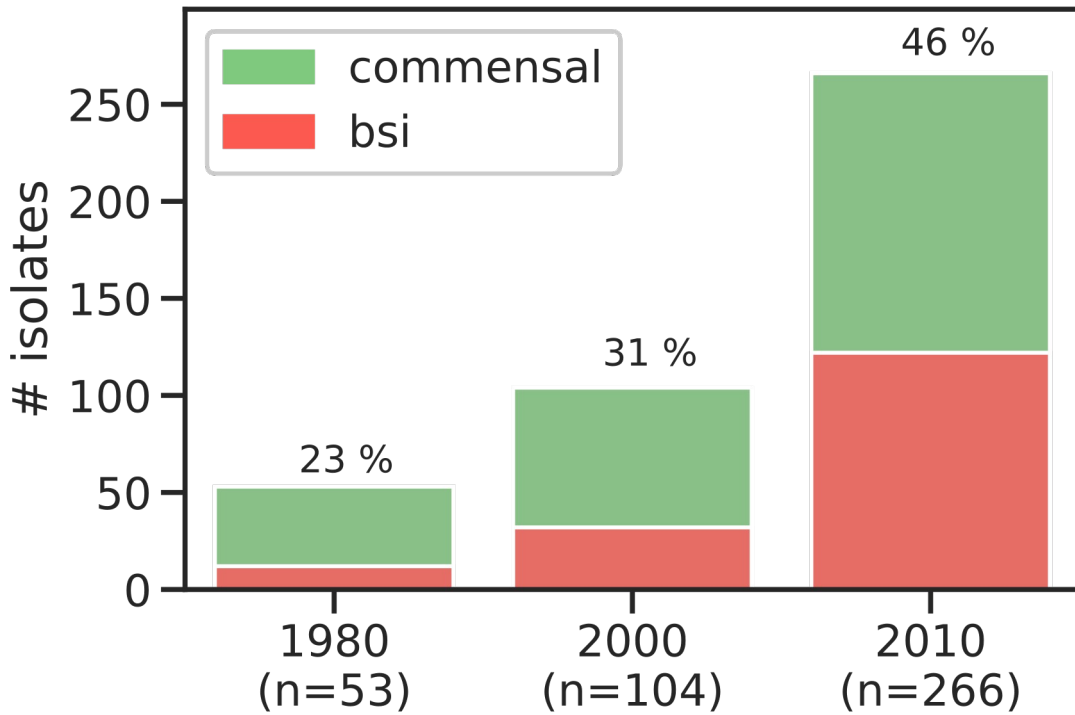


864 **Figure S2.** Predicted antibioresistance phenotypes of A) all the strains with a urinary portal of entry, (B) all the
865 strains with a digestive portal of entry, C) B2 strains, D) B2 strains with a urinary portal of entry and (E) B2
866 strains with a digestive portal of entry (Benjamini-Hochberg corrected p value < 0.05). The results are presented
867 as percentages of resistant strains for nine antibiotics of clinical importance. AMK, amikacin; AMP, ampicillin;
868 CARB, carbapenem; CTX/ CAZ, cefotaxime/ceftazidime; FEP, cefepime; FQ, fluoroquinolones; GEN,
869 gentamicin; SXT, cotrimoxazole; TZP, piperacillin/tazobactam. Significant differences are indicated by asterisks
870 (p value < 0.0001: ****; ns: non-significant).

871



872 **Figure S3. wg-GWAS model performance.** F1-score representation (blue dots), precision (yellow dots), and
873 recall (red dots). A) For the full collection B) the subset of clinical isolates with urinary tract as portal of entry,
874 and C) the subset of clinical isolates with digestive tract as portal of entry. The naive and the analysis with
875 covariates are represented. PE: portal of entry.



876 **Figure S4.** Proportion of BSI predicted isolates over time. 423 isolates from commensal collections were fitted
877 to the trained ML model. The proportion of BSI isolates for the 3 different periods of time is colored in red and
878 the percentage indicated above each bar. The total number of isolates per year is given in brackets.